Front. Earth Sci. 2017, 11(3): 579–591
DOI 10.1007/s11707-017-0640-5

RESEARCH ARTICLE

Modeling potential scenarios of the Tangjiashan Lake outburst and risk assessment in the downstream valley

Vera KIDYAEVA (✉)[1], Sergey CHERNOMORETS[1], Inna KRYLENKO[1], Fangqiang WEI[2,3], Dmitry PETRAKOV[1], Pengcheng SU[2], Hongjuan YANG[2], Junnan XIONG[2]

1 Lomonosov Moscow State University, Faculty of Geography, 119991 Moscow, Russia
2 Institute of Mountain Hazards and Environment, Chinese Academy of Sciences, Chengdu 610041, China
3 Institute of Green and Intelligent Technology, Chinese Academy of Sciences, Chongqing 400714, China

© Higher Education Press and Springer-Verlag Berlin Heidelberg 2017

Abstract This research is devoted to Tangjiashan Lake, a quake landslide-dammed lake, situated in Sichuan Province, China, which was formed by a landslide triggered by the Wenchuan Earthquake on 12 May 2008. A STREAM_2D two-dimensional hydrodynamic model of Russia was applied to simulate the process of two flood scenarios: 1, lake dam outbreak, and 2, dam overtopping. An artificial dam outbreak was made after the earthquake to lower the water level of the lake in 2008, which led to a great flood with a maximum water discharge of more than 6400 m^3/s. The negative impact of the flood was reduced by a timely evacuation of the population. Flood hazards still remain in the event of new landslides into the lake and lake dam overtopping (Scenario 2), in which case a maximum water discharge at the dam crest would reach 5000 m^3/s, placing the population of Shabacun and Shilingzi villages in the zone of flood impact.

Keywords Tangjiashan Lake, landslide-dammed lake outburst, hydrodynamic modeling, risk assessment

1 Introduction

Earthquakes and consequent slope failures such as rock- and landslides frequently form lakes or cascades of lakes in mountainous areas (Schuster and Alford, 2004; Owen et al., 2008). Failure of landslide dams typically happens within a short time after their formation. According to Schuster (1993), who studied 187 events worldwide, 55% of dams failed within 1 weak after their formation, whereas 89% failed after 1 year. Most fail by overtopping (if not artificially breached beforehand), whereas piping (internal seepage erosion) or slope failure of the dam itself is relatively rare (Korup, 2002). Being more or less stable, long-lived landslide dams could pose a threat to downstream populations and infrastructure, which considering the large volume of water, and its concentration in steep mountain terrain, could be significant (e.g., Schuster and Alford, 2004). Taking into account an increasing level of land-use activity observed in some mountain areas (Holub and Hübl, 2008; Stefanelli et al., 2015), mountain lake bursts might lead to significant losses and numerous victims (Couston et al., 2015; Champati Ray et al., 2016).

Landslide-dammed lakes are common in mountainous areas around the world, including the Himalayas (Shroder, 1998; Gupta and Sah, 2008; Runqiu, 2009; Champati Ray et al., 2016; Kargel et al., 2016; Ruiz-Villanueva et al., 2016), Central Asia (Schneider et al., 2011), New Zealand (Korup, 2002), the North American Cordillera (Clague and Evans, 1994; Hubbard et al., 2005), the Andes (Hermanns et al., 2004), the Caucasus (Chernomorets et al., 2007; Chernomorets, 2014), and other regions (Costa and Schuster, 1991). According to the research of Richardson and Reynolds (2000), over 50% of glacier lake outburst floods in the Himalayas are caused by displacement waves from different types of mass movements in lakes, i.e., by overtopping.

The highest earthquake-triggered rockslide dam in the world is located in the Murgab River, southeastern Tajikistan. The dam is 600 m high and forms Sarez Lake, which threatens thousands of people in downstream valleys (Schuster and Alford, 2004). One of the most realistic scenarios for a flood disaster downstream from the Sarez dam is considered to be an occurrence of an overtopping wave resulting from a landslide high on the right bank of Sarez Lake (Schuster and Alford, 2004). A flood from Vajont Reservoir was caused by a large

Received July 15, 2016; accepted January 25, 2017

E-mail: veramkid@gmail.com

landslide from Mount Toc, in Veneto (northern-eastern Italy), with estimated volume of 240–300 million m^3 (Guzzetti and Tonelli, 2004). Despite the fact that the dam was not destroyed, the displacement wave led to the dam overtopping and the resulting catastrophic flood killed at least 1900 people downstream (Genevois and Ghirotti, 2005).

In Chinese mountain ranges, formation of earthquake-triggered landslide-dammed lakes is quite common in Tibet (Han, 2003), Yunnan (Zhang et al., 2015) and Sichuan (Dai et al., 2005; Lee and Dai, 2011). One of the most important consequences of the Wenchuan Earthquake (in Sichuan) of 2008 was landslide-induced lake formation (Cui et al., 2009). Parts of the earthquake-induced landslides crashed into rivers to form landslide dams, which, in turn, formed landslide-induced lakes in the upper stream. The earthquake triggered 35 landslide-induced quake lakes, 34 of which were in Sichuan Province, forcing evacuations in some villages downstream from the affected rivers (Cui et al., 2009, 2012). Beichuan County was particularly affected by quake lakes, the largest being Tangjiashan Lake.

Although the lake has been quasistable since the earthquake, high-magnitude earthquakes are highly probable in this region, and they can provoke landslides into the lake that could cause displacement waves and dam overtopping and failure (Kafle et al., 2016). Based on the Vajont event experience (Guzzetti and Tonelli, 2004; Bosa and Petti, 2013), reinforcing of the Tangjiashan Lake dam does not completely prevent the risk of flood in the downstream valley. Thus, a mitigation strategy for flood hazards should be developed and a risk assessment for the downstream valley must be integrated to the strategy.

Spatially, this study focuses on Tangjiashan Lake and the Jianjiang River Valley, with a total length of 27 km downstream from the lake dam. The goal of the study is to assess hazard and social risk for a case of dam overtopping or failure. The following tasks were undertaken to achieve the study's aim: assessment of the lake volume and downstream terrain; modeling of the lake outburst based on two hazardous scenarios; hazard zonation in the Jianjiang River Valley; a vulnerability assessment and estimation of social risk for the downstream population.

2 Background

2.1 Tangjiashan Lake

Tangjiashan Lake is located at 31°50′57″N and 104°25′31″E on the Jianjiang (Tongkou) River. It is a quake lake only 6 km upstream from Beichuan City, and 70 km from Mianyang City (Fig. 1), with population of more than four million people. Its maximum storage capacity, evaluated after the lake formation, was about 3.16×10^8 m^3 (Liu et al., 2009).

Tangjiashan Lake was formed in 2008 as a result of the Wenchuan Earthquake. This case study is relevant due to the high probability of secondary earthquakes in the region, which might cause destruction of the dam or/and a rockslide into the lake. The lake is located in a densely populated mountainous region of Sichuan. The cities of Mianyang, with a population of 4.6 million people (70 km away), Beichuan, destroyed by the earthquake (8.5 km

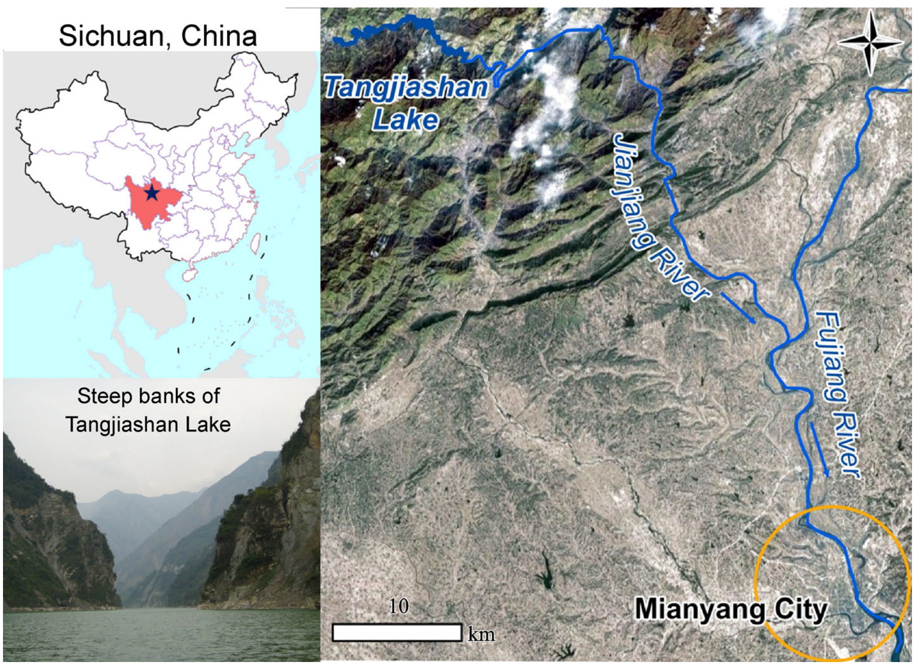

Fig. 1 Tangjiashan Lake and Jianjiang River Valley (background image: Landsat ETM +, photo by: V. Kidyaeva).

away), approximately 40 villages, four large hydraulic structures (the Kuzhuba, Tongkou, Tongkouhe, and Qinglian dams), and several major bridges and highways are situated downstream from the lake. Moreover, the study allows researchers to follow the formation and evolution of a landslide-dammed lake almost since its inception.

Tangjiashan Lake was originally highly unstable, threatening 1.3 million people downstream, and necessitating the evacuation of 250,000 people from Mianyang City as authorities worked to stabilize the dam. The bedding landslide was composed of weathered schist and slate with sand; the height difference of the anterior and posterior part of the landslide reached 650 m and the horizontal distance covered by it was approximately 1250 m (Liu et al., 2009).

In early June 2008, excavations were made in the dam to a slotting depth of 20 m. The upstream water level of Tangjiashan Lake achieved its highest water level of 743.10 m above sea level (a.s.l.) on 10 June 2008 and then fell back to 719.48 m a.s.l. later the same day, thus meeting a dam's safety design standards (Chen et al., 2011). After this positive event, plans to build a hydropower station came under consideration.

The length of the Tangjiashan Dam along the river was 803.4 m; the width of the dam, 611.8 m; its area, 0.31 km^2; and its volume, 2037×10^4 m^3 (Liu et al., 2009). The dam rose above the river to heights between 82 and 124 m, its maximum elevation was 793 m a.s.l., and the base was located at 669 m a.s.l. (Chen et al., 2011).

2.2 Jianjiang River

The total Jianjiang River drainage area measures 4520 km^2, and it is a tributary of the Fujiang River and is related to the Yangtze Basin. According to Chen et al. (2011), the drainage area upstream from the Tangjiashan Dam measures 3550 km^2. The length of the river is 173 km, in the location of the dam the river's width was 100–130 m, its depth was 0.5–2 m, and its low water level was 664.8 m (Liu et al., 2009). Mean annual discharge of the river is 1600 m^3/s (Chen et al., 2011).

In the Jianjiang River Valley, where the lake is located, rains are dominant from May to September (accounting for approximately 86.3% of the annual precipitation). According to the Beichuan meteorological station, the average annual rainfall in the basin is 1355.4 mm, and the maximum recorded daily maximum is 323.4 mm (Liu et al., 2009). According to Tan and Hen (1992), in the Longmenshan area the intensity of a rainfall that can initiate debris flows must be greater than 30–50 mm/h, with a total rainfall amount of at least 80–100 mm (Adegbe et al., 2013).

The width of the river at the modeling site is from 80 m to 100 m (Tang et al., 2012). The widest part (up to 300 m) is located near the village of Xuantouba, at the confluence of the major left tributary. The width of the lower part of the valley, including the floodplain and floodplain terraces, is up to 2 km. The downstream modeling target is located on the hydroelectric dam at Tongkou (Fig. 2).

The Jianjiang River Valley is densely populated, with more than 40 villages and small towns downstream from the lake. Four artificial dams were built in this part of the valley; one of them, the Kuzhuba Dam, could not withstand the earthquake and was covered by sediments. The area specializes mainly in agriculture and crop planting, with fields and gardens located within the floodplain.

2.3 Artificial dam-break of Tangjiashan Lake and corresponding flood on Jianjiang River

After the formation of Tangjiashan Lake, great efforts were made to stabilize and lower the lake's water level. First, after channel construction, the flow from the lake began at 7 June 2008, but over the next 2 d, the discharge did not increase. The discharge began to increase rapidly after the lake's water level reached 743.1 m a.s.l. at 1:30 CST on 10 June 2008 (Huang et al., 2012). Maximum outbreak discharge was 6420 m^3/s at 10:00 CST on 10 June 2008 (Zhang, 2010; Chen et al., 2011) (Fig. 3), after which the water level began to fall and the bottom of the channel began to erode. At 8:00 CST on 11 June 2008, the water level dropped to 715 m a.s.l., the water flow decreased to 79 m^3/s, the erosion stopped, and the lake reached a conditionally stable state (Zhang, 2010; Chen et al., 2011). The maximum volume of the lake after dam-break reached 2×10^8 m^3 (Chen et al., 2011), or, according to other estimates, 2.29×10^8 m^3 (Xu et al., 2009).

The data from field observations of the dam-breakdown process and the outburst flood passage in the valley, described in Zhang (2010), allowed us to set the task of modeling the process and calibrate the resulting model. Observations of the flood were conducted at two points in the valley: at the hydrological station downstream from Beichuan City and at the Tongkou hydroelectric dam (Zhang, 2010) (Table 1).

The maximum water discharge in Beichuan was observed 30 min after it passed through the target of the dam, which meant that the average velocity of the moving flood wave was 4.86 m/s. In Tongkou, the maximum discharge was observed after 1 h and 24 min past Beichuan; therefore, the average flow velocity was 3.58 m/s (Zhang, 2010).

3 Methods

3.1 Field campaign in the study area

Tangjiashan Lake and the Jianjiang River Valley were investigated by a group of scientists from the Institute of

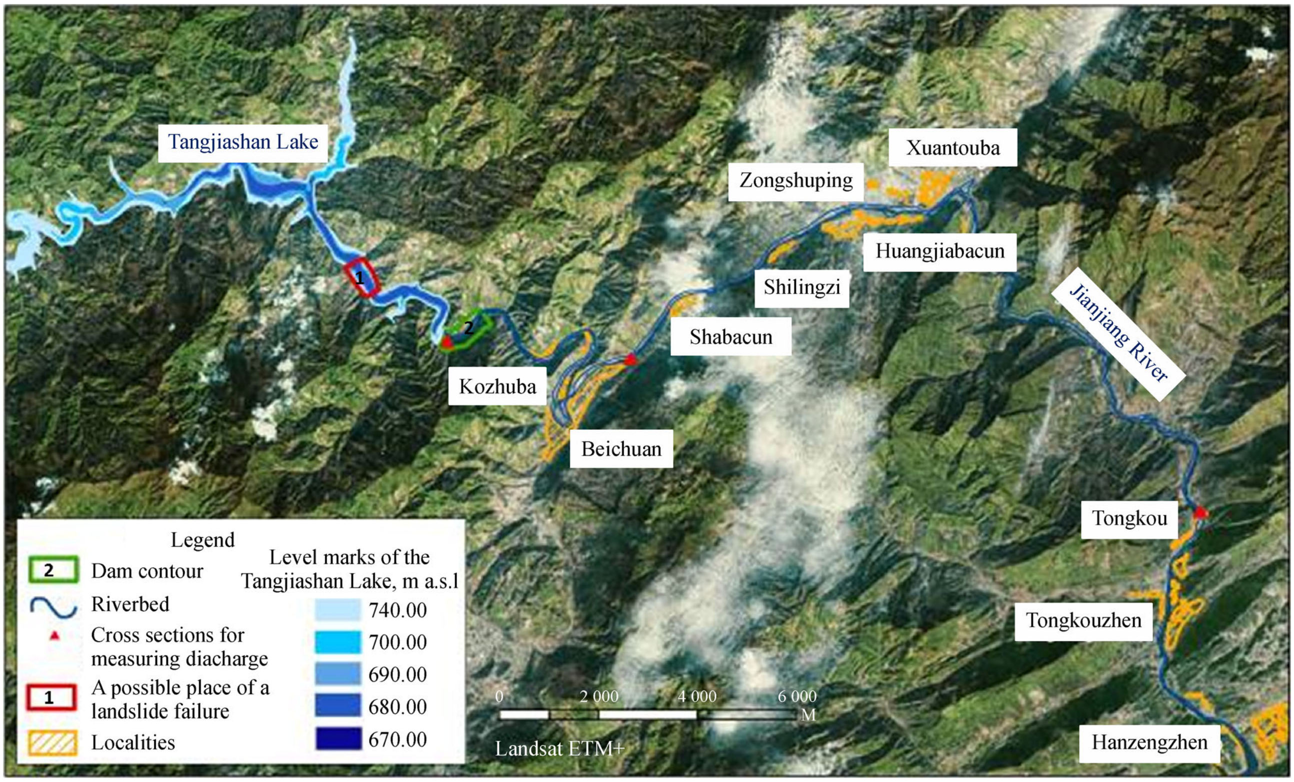

Fig. 2 Jianjiang River Valley, including villages (background image: Landsat ETM +).

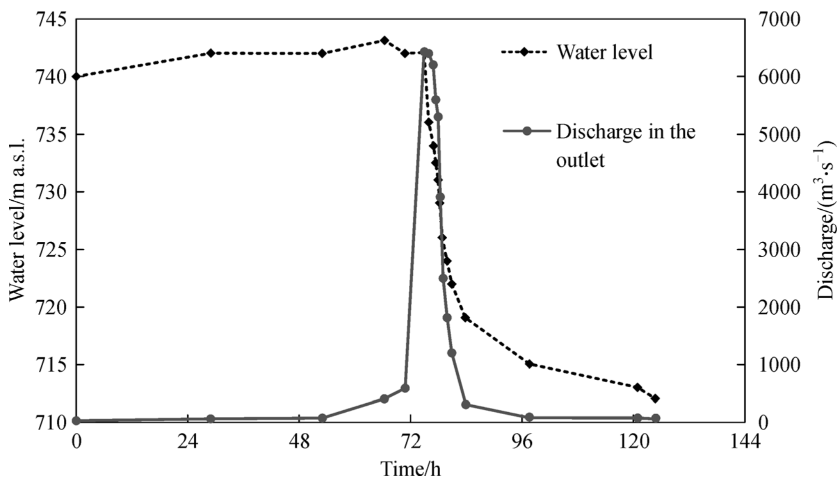

Fig. 3 Outburst hydrograph data during the artificial dam failure in June 2008 (Chen et al., 2011; Zhang, 2010).

Table 1 Measured peak discharges and corresponding occurrence times (Zhang, 2010)

Position	Distance from Tangjiashan Dam/km	Peak discharge $/(m^3 \cdot s^{-1})$	Occurrence time
Tangjiashan Dam	0	6500	12:30 CST
Beichuan hydrologic station	4.6	6540	12:50 CST
Tongkou hydrologic station	26.0	6210	13:50 CST

Mountain Hazards and Environment, Chinese Academy of Sciences (China) and from Lomonosov Moscow State University (Russia), both in October 2010 and in May 2011. Field work was divided into two parts. The first part was held in October 2010, when the volume of Tangjiashan Lake was measured. Bathymetric surveying was done using a motorboat and a Lowrance 525 CF two-ray echo sounder which has been successfully applied to the study of landslide-dammed lakes in China (Zhang et al., 2015) and which produces echograms of georeferenced data. The volume and average depth of the lake were calculated using ArcGIS software (Esri, USA). This was the first time the volume and depth of the lake were measured instrumentally.

The Jianjiang River Valley field research was held in May 2011. Investigations were conducted in the Jianjiang and Fujiang River valleys. Differential GPS devices [Trimble (USA) and Contour XLRic (GeoSolution, USA)] were used to survey the downstream area and to take measurements of the dam elevation. As a result, more than 3000 points with coordinates and elevations were obtained and were used to detail the topography. Reconnaissance was carried out to locate the villages, the most important landslides, bridges, and artificial dams, as well as bank protection dams; the river width was measured, and morphometric characteristics of the artificial dams were obtained.

Data concerning the population of the valley were assessed via remote methods, for example, by calculating the number of buildings in the small villages and assessing the number of their inhabitants using time transgressive satellite imagery from Google Earth.

3.2 Hydrodynamic modeling

The main characteristics of the flow intensity, which can be used for the hazard zoning of river valleys, are flow velocity and depth. For evaluation of these characteristics, two-dimensional hydrodynamic modeling of water flow movement was used.

Two-dimensional models of water flow are based on numerical solution of the Saint-Venant equations, also known as “the shallow water equations” (Cunge et al., 1980). Detailed information about the topography of the river valleys is necessary for model setup. For the numerical solution of the equations, the boundary and initial conditions must be specified. The boundary conditions are water discharges on the upper boundaries and water levels at the lower boundary of the computational domain as a function of time. The initial conditions are the water surface levels within the modeling area, taken at the beginning of the calculation. As a result of modeling, one can determine a spatial distribution of the mean average flow velocities, water surface levels, and water depths within the computational domain.

Modeling of the outburst floods was conducted using the STREAM_2D software package (Belikov and Militeev, 1992; Belikov et al., 2015). The software is based on the numerical solution of the two-dimensional equations of water flow on the basis of irregular triangular-quadrilateral hybrid computational grids. This excluded the opportunity to explore the possible transformation of floods into debris floods (STREAM_2D does not consider debris movement), but, nevertheless, made it possible to investigate the flooding of valleys and main flood characteristics.

As input data for modeling, we used bottom relief based on digital elevation model (DEM), prepared in accordance with a map scale of 1:10,000. A digital terrain model was partially corrected using field survey data, which reflected changes in topography after the earthquake.

Modeling of the outburst flood propagation was conducted in the area of the valley 27 km downstream from Tangjiashan Lake for two scenarios. The first scenario is based on a lake outburst event case after an earthquake in June 2008. The second scenario assumes the stability of the lake up to the destruction of the dam and flood formation by the large landslide failure, which, in the case of falling close enough to the dam, can cause an overflow wave. Both the lake and downstream valley were included in the computational domain in this case. A likely unstable part of the lake shore, located approximately 3 km from the dam alignment, was chosen as a location of landslide failure (Fig. 2). The possible collapse of the volume was set at 1×10^6 m^3. The overflow hydrograph was calculated as follows: two datasets with the bottom relief were prepared. The first was unchanged and the second one had an elevation that would have existed after the landslide failure in the lake. During the calculations, the first dataset was replaced by the second without interrupting the calculation process. As a response to the bottom configuration change, a hydrograph was obtained, showing the discharge of water displacement waves at Tangjiashan Dam (Fig. 4) (Krylenko and Kidyaeva, 2012). The maximum calculated flow discharge was about 5000 m^3/s, the bulk of the water passed through the dam in 10 min, and repeated waves took place in the next 10–15 minutes and were relatively small — up to 500 m^3/s (Fig. 4).

3.3 Risk assessment method

According to the common approach, a risk assessment consists of two parts: hazard assessment and vulnerability assessment (Reynolds, 2003; Birkmann, 2006; Fuchs et al., 2012 and others). Typically, risk is calculated as a multiplication of *hazard* and *vulnerability*.

In the case study, we assumed that a natural *hazard* is a threatening event with an indication of the place and time of its development, which is determined by the entire complex of natural conditions that affect the *probability* of a hazard and its *intensity* (https://www.unisdr.org).

Flood *probability* cannot be calculated for this research directly because of a lack of data. For such statistical calculations, long series of data on the occurrence of the outbursts are required; this is not possible because the lake was formed only in 2008. Another way to assess probability is to calculate the probability of outbursts for the particular type of lake throughout the region (“spatial probability”); however, these data are also unavailable. Therefore, we assumed that the hazard of the second scenario is only a potential hazard, because it is not defined precisely in time.

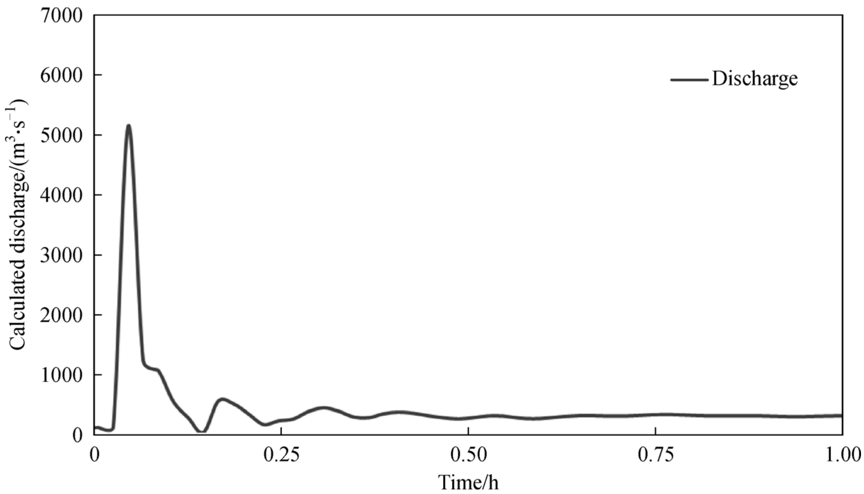

Fig. 4 Calculated hydrograph for the Scenario 2 (Krylenko and Kidyaeva, 2012). The smoothed line is obtained by a large amount of calculated points (more than 600).

Table 2 Classes of intensity according to prior demolition of buildings. Adapted from the Russian EMERCOM statistics (EMERCOM, 2003)

Class of intensity	1	2	3	4	5
$P/(\mathrm{kg}\cdot\mathrm{s}^{-2})$	< 62.5	62.5 –1000	1000 –4500	4500 –171500	> 171500
Demolitions	None; washing out of the agriculture land is possible	Low	Medium	High	Catastrophic

Floods typically pose a threat due to long-term inundation and damage to buildings and infrastructure from impact of the water stream (García et al., 2003). Taking into account that long-term inundation is not typical for lake bursts, we assumed that a major hazard is driven by flood severity or intensity. Typically, flood *intensity* is defined by the function of both flow depth and velocity (O'Brien et al., 1993). In other words, the intensity of the flood is the specific energy of the flood (P, in kg/s^2) (EMERCOM, 2003):

$$P = 0.5\rho HV^2, \quad (1)$$

where ρ is the density of the flow (water, debris flow, or mud flow), H – the depth of the flow, and V – the velocity of the flow. All of these data were obtained from the modeling results.

The range of the flood intensity is very wide — from zero to several hundred thousand kg/s^2. The flood intensity range is usually divided into classes of high, middle, and light danger (Wei et al., 2003). We divided the range into five classes according to the prior degree of demolition (Table 2). Demolitions of different types of buildings are published in the Russian EMERCOM (The Ministry of the Russian Federation for Civil Defence, Emergencies and Elimination of Consequences of Natural Disasters) method (EMERCOM, 2003, 2007).

The social vulnerability assessment is calculated according to the EMERCOM method for exposed populations (EMERCOM, 2003; Zemtsov et al., 2016), based on statistics of demolitions, victims, and casualties of floods in Russia for floods of different intensity. Taking into account that in the World Risk Index (Garschagen et al., 2015) the ratings of Russia's and China's vulnerability are very close (41 and 47.10, respectively), the assumption was made that the statistics of hazardous flood consequences for these countries is similar.

The method is based on dividing the exposed area into five zones (Table 3). Zones of impact with high reliability can be correlated with classes of intensity as proposed in Table 2. The flood with a first class of intensity does not cause casualties. Parameters in Table 3 are normative coefficients of population vulnerability.

The next step entails calculating the number of victims — the social risk. We used GIS to assess the share of each inhabited locality's area covered by each of the five zones of impact. For each zone, the total number of inhabitants was calculated and then, using Table 3, the number of potential dead and injured inhabitants was assessed for both day and night situations. For the estimations for the first scenario, the satellite image dated April 2005 was used; for the second, that of January 2010 was used.

4 Results

4.1 Tangjiashan Lake morphometry

According to the measurements, the characteristics of Tangjiashan Lake in October 2010 were as follows:

Table 3 Percentage of victims and casualties in different zones of flood. Adapted from the Russian EMERCOM statistics (EMERCOM, 2003)

Zone of impact	Total losses/(% of population)		From total losses			
			Dead/%		Injured/%	
	Day	Night	Day	Night	Day	Night
1 – no impact	0	0	0	0	0	0
2 – low impact	2	10	5	10	95	90
3 – medium impact	5	15	7	15	93	85
4 – high impact	13	25	10	20	90	80
5 – catastrophe	60	90	40	75	60	25

volume (W) 67.8×10^6 m^3, maximum depth (h_{max}) 41.2 m, area (F) 4.03×10^6 m^2, and length (l) 14×10^3 m (Fig. 5). In 2008, when the lake appeared, its volume was 3.5 times larger than in 2010.

4.2 Model validation

The results of the calculations for the first scenario were used for model calibration and adjustment of the relief. The outburst flood hydrographs in the control cross-sections were compared to the results of discharge measurements, published in Zhang (2010).

Maximum simulated water discharge in the Beichuan cross-section was 6390 m^3/s, which is slightly below the measured value, and in the Tongkou cross-section it was 6270 m^3/s, which is almost identical to the measured value. Figure 6(a) shows a comparison of the simulated and measured hydrographs in the Beichuan cross-section, and the input hydrograph at the dam cross section. The figure shows the form of hydrograph transformation that occurred. The result for the Tongkou cross-section is slightly worse (Fig. 6(b)).

The lag time between the Beichuan and Tongkou cross-sections was 50 min, which is almost 30 min less than it was in reality, showing that the velocities were overestimated in this area. In reality, the outburst flood met many objects, such as landslide dams and lakes, which hampered the roughness of the river bed but were not taken into account in the simulation. Consequently, in further calculations the roughness coefficient between the cross-sections was corrected.

4.3 Flood parameters for potential Tangjiashan Lake burst

The maximum depth of the flood in case of an overtopping wave in the second scenario was observed at the dam and 1 km downstream, and it reached up to 18.7 m (Fig. 7(a)). In the Beichuan cross-section the maximum calculated depth was 5 m. Near Dengjiadu and Xuantouba villages, the depth decreased to 2–3 meters and water flooded a rather flat bottom of the valley, including Shilingzi village and partially Zongshuping village. Downstream, near

Fig. 5 Tangjiashan Lake depth according to bathymetric surveys (background image: Landsat ETM +).

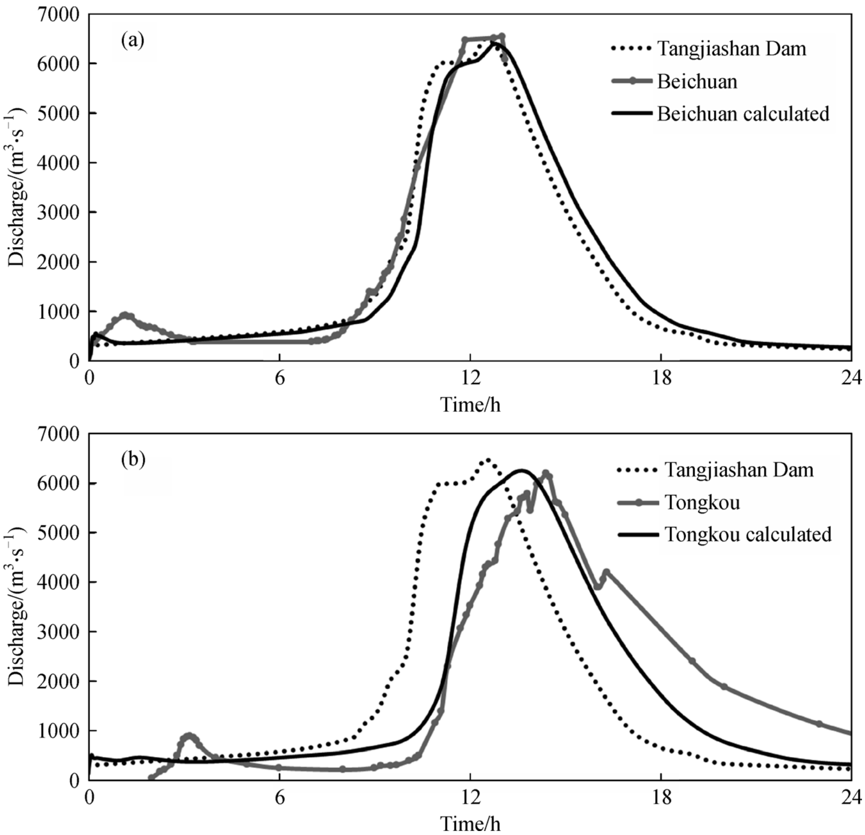

Fig. 6 Comparison of observed and calculated hydrographs for (a) Beichuan and (b) Tongkou cross-sections.

Xuantouba village, the wave lost its intensity. Despite the relatively narrow valley, the depth in this area did not exceed 4 m (Fig. 7(a)).

Maximum flow velocities were high. According to the modeling results, at Tangjiashan Dam they reached 13.7 m/s (Fig. 7(b)). Downstream, the dam maximum velocities reached 4–5 m/s in the narrowest parts of the valley, while in other parts of the valley the maximum velocities were less than 3 m/s (Fig. 7(b)).

4.4 Social risk assessment in the downstream valley

According to the calculations, the first scenario is the most hazardous due to the highest discharge, and the greater number of potentially flooded territories and the possible water levels rising at the locations of the towns. It was estimated that approximately 441 people could potentially lose their lives during a flood during the day; the number increases to 1538 during the night. Total losses were evaluated as 1979 lives lost during daytime and 3544 during nighttime (Table 4). The table shows the possible number of victims and casualties that could have occurred during the outburst flood in 2008; fortunately, according to authorities, no fatalities were reported. When the excavation of the dam was planned by the authorities, all inhabitants in the downstream towns and cities were evacuated.

The social risk of the second scenario tends to be less dramatic, due to lower water discharge, lower velocities, and lower water levels. It is necessary to take into consideration that many localities, such as Beichuan and Kuzhuba, are no longer populated after the earthquake. Other localities, such as Xuantouba, moved to the upper slopes of the valley and are no longer accessible by the river flow. Analysis of the latest satellite images showed that most exposed to future possible floods are houses in Shabacun and Shilingzi villages. Some of the territory of both villages are still located in the flooded area of low and medium impact (Fig. 8). According to our investigation, there could be approximately 100 casualties in these villages during the day and 150 at night in the event of the Tangjiashan Lake dam overtopping and a corresponding flood event.

5 Discussion

The choice of 2D model was justified by the quantity and quality of input data as well as the assessment's accuracy requirement. We also note that 2D models are widely used for simulation of outburst floods in mountain areas around the world (Worni et al., 2014). A 1D model could not

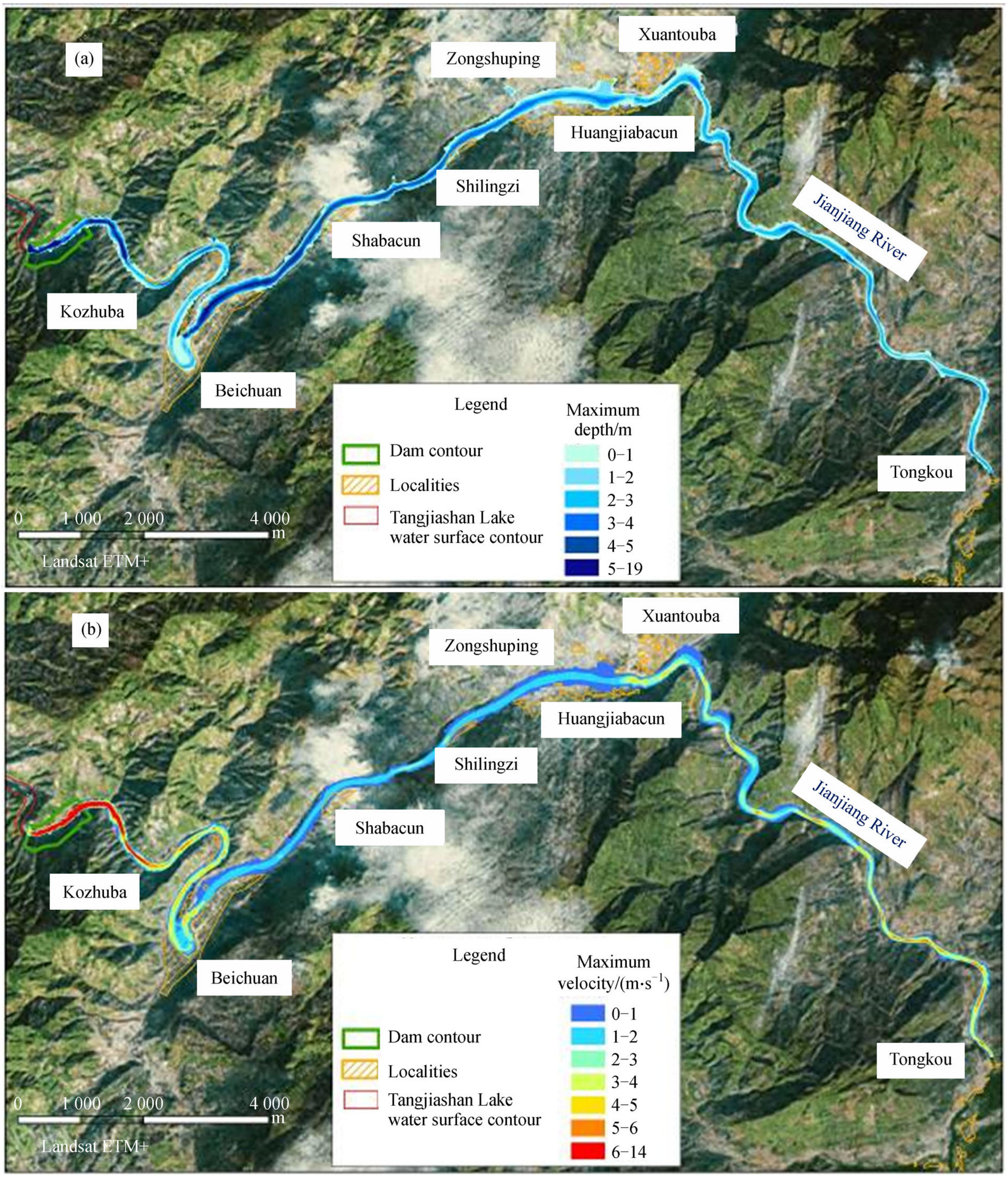

Fig. 7 (a) Maximum depth and (b) flow velocity of flood according to Scenario 2 (background image: Landsat ETM +).

provide the spatial pattern of flow parameters, i.e., water depth and flow velocity. 3D modeling requires more input data, such as more detailed topography and additional data about the vertical distribution of flow characteristics for model calibration, and thus could not be realized in our case. A 1D-2D hydrodynamic model has been already used to simulate the spatial variations in flood parameters in this valley and has shown satisfactory results (Fan et al., 2012).

There are many state-of-the-art models based on the numerical solution of the Saint-Venant equations (MIKE21, FLO-2D, and Delft3D among others). For our research, we used STREAM_2D software, which is widely used in Russia. It is based on irregular triangular-tetragonal hybrid grids that allow adapting the model for areas where flow configuration is complicated. STREAM_2D (and its previous modification, RIVER) has been widely applied

Table 4 Number of victims and casualties in the localities exposed to flooding

Zone of impact	Total losses				From total losses							
					Dead				Injured			
	Day		Night		Day		Night		Day		Night	
	Sc1[a)]	Sc2[b)]	Sc1	Sc2	Sc1	Sc2	Sc1	Sc2	Sc1	Sc2	Sc1	Sc2
Beichuan	1089	0	2175	0	108	0	423	0	981	0	1752	0
Dengjiadu	459	0	705	0	172	0	488	0	287	0	217	0
Houses along the river	1	0	3	0	0	0	1	0	1	0	2	0
Kozhuba	7	0	13	0	1	0	3	0	6	0	10	0
Shabacun	120	60	180	90	48	3	135	9	72	57	45	81
Shilingzi	120	40	180	60	48	3	135	9	72	37	45	51
Xuantouba	183	0	288	0	64	0	182	0	119	0	106	0
Total	1979	100	3544	150	441	6	1367	18	1538	94	2177	132

a) Sc1 denote Scenarios 1; b) Sc2 denote Scenarios 2.

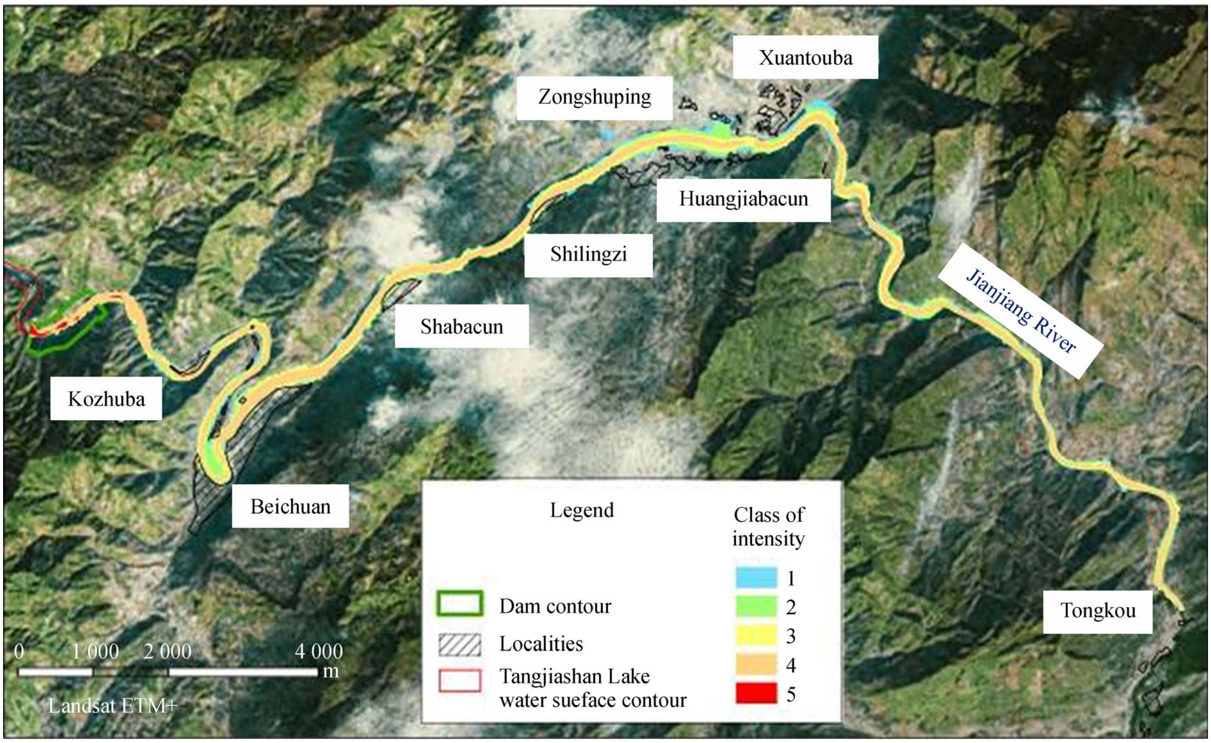

Fig. 8 Intensity zoning in the Jianjiang River Valley according to Scenario 2 (background image: Landsat ETM +).

for flood simulation for many rivers in different natural conditions and flood plains, e.g., the Volga, Amur, Ob, Lena, etc. (Belikov et al., 2015), as well as in mountain areas (Petrakov et al., 2012). STREAM_2D software includes a dam-break module and gives stable solutions in cases of highly nonstationary flow, such as outburst floods; it was implemented for flood hazard zonation in the case of dam breaks for major Russian reservoirs.

Considering that the water volume in Tangjiashan Lake is comparable with that of a large reservoir, we simulated a potential outburst flood from the lake like a similar event (Bosa and Petti, 2013). For the case of steep mountain terrain, a transformation of an outburst flood into debris flow could occur (Ruiz-Villanueva et al., 2016). Owing to the large lake volume, high discharge of outburst flood, and low channel angle for most of the flood route, the probability of this occurrence is very low. During artificial lake drainage in 2008 with a discharge similar to that simulated, debris flow or debris flood was not observed. Thus, we did not take into account the probability of debris flow or debris flood.

The parameters of the flow during an artificial outburst in 2008 (Scenario 1) characterize the possible maximum of flood intensity in the Jianjiang River Valley and corresponding social risk. In case of possible overflow over the dam (Scenario 2), as result of a new landslide the maximum discharge will be about 5000 m^3/s, which is less than the maximum discharges during the artificial outburst in 2008 (7000 m^3/s). We note that similar triggers are considered for scenario of lake outbursts in future (Schuster and Alford, 2004) or caused catastrophic floods downstream in the past (Genevois and Ghirotti, 2005). The risk in the case of realizing Scenario 2 is less, but it still exists and should be taken into account for planning economic activity in the valley. We also simulated other scenarios, such as landslides and rockslides into more remote parts of the lake. In this case, the overflow discharge was up to 1000 m^3/s, which is significantly lower compared to Scenarios 1 and 2.

A scenario of dam failure due to seepage or overtopping was not considered because the dam has been reinforced and has significant width. It agrees with existing assessments for similar dams (for example, Korup, 2002). Nevertheless, monitoring of the dam should be continued to exclude this cause of failure in the future.

If no high-magnitude earthquakes occur in the vicinity of the lake, we expect that the volume of the Tangjiashan Lake will decrease due to sedimentation. Assuming the mean Jianjiang River discharge at Tangjiashan Lake to be 100 m^3/s and the mean sediment discharge to be 100 kg/s, we can predict that the lake could be completely filled in by sediment in 40 yr.

6 Conclusions

The situation in Beichuan County from May to June 2008 can be characterized by a sequence of several disasters: earthquake, landslides, rockfalls, and outburst floods. The aim of this research was to only assess the risk pertaining to Tangjiashan Lake outburst or overflow. Results of modeling an artificial dam outbreak (Scenario 1) showed good correspondence with observation data. Appropriate mitigation measures in 2008 (dam cutting and population evacuation) provided an opportunity to guard against the occurrence of a hazardous situation The risk of dam overtopping due to a landslide into the lake (Scenario 2) still remains to be investigated. The maximum outflow discharge in this case according to our estimations would reach 5000 m^3/s, and Shabacun and Shilingzi villages would be in the flooded area at low and medium hazard levels.

Acknowledgements The study was partially supported by the Science and Technology Support Project of Sichuan Province (No. 2015SZ0214), by the International Cooperation Project of the Ministry of Science and Technology of China (No. 2009DFR20620), and by Russian Foundation for Basic Research (RFBR) Research Project Nos. 14-05-00768 and 15-05-06894.

References

Adegbe M, Alkema D, Jetten V G, Agbor A T, Abdullahi I D, Shehu O U, Unubi A S (2013). Post seismic debris flow modelling using Flo-2D; case study of Yingxiu, Sichuan Province, China. Journal of Geography and Geology, 5(3): 101–115 doi:10.5539/jgg.v5n3p101

Belikov V, Militeev A (1992). Two-layer mathematical model of catastrophic floods. Computing Technologies, 1(3): 167–174 (in Russian)

Belikov V V, Krylenko I N, Alabyan A M, Sazonov A A, Glotko A V (2015). Two-dimensional hydrodynamic flood modelling for populated valley areas of Russian rivers. In: Proceedings IAHS, Changes in Flood Risk and Perception in Catchments and Cities, 370: 69–74

Birkmann J, Dech S, Hirzinger G, Klein R, Klüpfel H, Lehmann F, Mott C, Nagel K, Schlurmann T, Setiadi N J, Siegert F, Strunz G (2006). Measuring vulnerability to promote disaster-resilient societies: conceptual frameworks and definitions. In: Birkmann J, ed. Measuring Vulnerability to Natural Hazards: Towards Disaster Resilient Societies. Tokyo: UNU-Press, 1: 9–54

Bosa S, Petti M (2013). A numerical model of the wave that overtopped the Vajont dam in 1963. Water Resour Manage, 27(6): 1763–1779

Champati Ray P K, Chattoraj S L, Bisht M P S, Kannaujiya S, Pandey K, Goswami A (2016). Kedarnath disaster 2013: causes and consequences using remote sensing inputs. Nat Hazards, 81(1): 227–243

Chen X Q, Cui P, Li Y, Zhao W Y (2011). Emergency response to the Tangjiashan landslide-dammed lake resulting from the 2008 Wenchuan Earthquake, China. Landslides, 8(1): 91–98

Chernomorets S S (2014). New “Kazbek Obstruction” of 17 May 2014. Priroda, 7: 67–72 (in Russian)

Chernomorets S S, Tutubalina O V, Seinova I B, Petrakov D A, Nosov K N, Zaporozhchenko E V (2007). Glacier and debris flow disasters around Mt. Kazbek, Russia/Georgia. In: Chen C L, Major J J, eds. Proceedings 4th International Conference on Debris-Flow Hazards Mitigation—Mechanics, Prediction, and Assessment. Rotterdam: Millpress, 691–702

Clague J J, Evans S G (1994). Formation and failure of natural dams in the Canadian Cordillera. Geological Survey of Canada Bulletin, 464: 1–35

Costa J E, Schuster R L (1991). Documented historical landslide dams from around the world. U.S. Geological Survey Open-File Report 91-239. https://pubs.usgs.gov/of/1991/0239/report.pdf

Couston L A, Mei C C, Alam M R (2015). Landslide tsunamis in lakes. J Fluid Mech, 772: 784–804

Cui P, Dang C, Zhuang J Q, You Y, Chen X Q, Scott K M (2012). Landslide-dammed lake at Tangjiashan, Sichuan Province, China (triggered by the Wenchuan Earthquake, May 12, 2008): risk assessment, mitigation strategy, and lessons learned. Environ Earth Sci, 65(4): 1055–1065

Cui P, Zhu Y Y, Han Y S, Chen X Q, Zhuang J Q (2009). The 12 May Wenchuan earthquake-induced landslide lakes: distribution and preliminary risk evaluation. Landslides, 6(3): 209–223

Cunge J A, Holly F M Jr, Verwey A (1980). Practical Aspects of Computational River Hydraulics. Boston, London, Melbourne: Pitman

Dai F C, Lee C F, Deng J H, Tham L G (2005). The 1786 earthquake-triggered landslide dam and subsequent dam-break flood on the Dadu River, southwestern China. Geomorphology, 65(3–4): 205–221

EMERCOM (2007). The method for determining of the damage that can affect life and health of persons, property of people and entities as a result of shipping waterworks accident. Approved by the Order of the Ministry of the Russian Federation for Civil Defence, Emergencies and Elimination of Consequences of Natural Disasters and the Ministry of Transport of the Russian Federation on 2 October 2007, No. 528/143. Moscow (in Russian)

EMERCOM (2003). The method for determining of the damage that can be caused to life and health of persons, property of people and entities as a result of combustive power-producing civil engineering works accidents. Approved by the Order the Ministry of the Russian Federation for Civil Defence, Emergencies and Elimination of Consequences of Natural Disasters and the Ministry of Energy of the Russian Federation on 29 December 2003, No. 776/508. Moscow (in Russian)

Fan X, Tang C X, van Westen C J, Alkema D (2012). Simulating dam-breach flood scenarios of the Tangjiashan landslide dam induced by the Wenchuan Earthquake. Nat Hazards Earth Syst Sci, 12(10): 3031–3044

Fuchs S, Birkmann J, Glade T (2012). Vulnerability assessment in natural hazard and risk analysis: current approaches and future challenges. Nat Hazards, 64(3): 1969–1975

García R, Lopez J L, Noya M, Bello M E, Bello M T, Gonzalez N, Paredes G, Vivas M I, O'Brien J S (2003). Hazard mapping for debris flow events in the alluvial fans of northern Venezuela. In: Rickenmann D, Chen C, eds. Third Int Conf on Debris-Flow Hazards Mitigation: Mechanics, Prediction, and Assessment. Rotterdam: Millpress, 589–599

Garschagen M, Hagenlocher M, Kloos J, Pardoe J, Lanzendörfer M, Mucke P, Radtke K, Rhyner J, Walter B, Welle T, Birkmann J (2015). World risk report 2015. Bündnis Entwicklung Hilft and United Nations University Institute of Environment and Human Security (UNU-EHS), Bonn

Genevois R, Ghirotti M (2005). The 1963 Vajont Landslide. G Geol Appl, 1: 41–52

Gupta V, Sah M P (2008). Impact of the Trans-Himalayan Landslide Lake Outburst Flood (LLOF) in the Satluj catchment, Himachal Pradesh, India. Nat Hazards, 45(3): 379–390

Guzzetti F, Tonelli G (2004). Information system on hydrological and geomorphological catastrophes in Italy (SICI): a tool for managing landslide and flood hazards. Nat Hazards Earth Syst Sci, 4(2): 213–232

Han Z H (2003). Large-scale landslide-debris avalanche in Tibet, China. Landslide News, 14/15: 22–23

Hermanns R L, Niedermann S, Ivy-Ochs S, Kubik P W (2004). Rock avalanching into a landslide-dammed lake causing multiple dam failure in Las Conchas valley (NW Argentina) –Evidence from surface exposure dating and stratigraphic analyses. Landslides, 1(2): 113–122

Holub M, Hübl J (2008). Local protection against mountain hazards—State of the art and future needs. Nat Hazards Earth Syst Sci, 8(1): 81–99

Huang Y, Chen W, Liu J (2012). Secondary geological hazard analysis in Beichuan after the Wenchuan earthquake and recommendations for reconstruction. Environ Earth Sci, 66(4): 1001–1009

Hubbard B, Heald A, Reynolds J M, Quincey D, Richardson S D, Luyo M Z, Portilla N S, Hambrey M J (2005). Impact of a rock avalanche on a moraine-dammed proglacial lake: Laguna Safuna Alta, Cordillera Blanca, Peru. Earth Surf Process Landf, 30(10): 1251–1264

Kafle J, Pokhrel P R, Khattri K B, Kattel P, Tuladhar B M, Pudasaini S P (2016). Landslide-generated tsunami and particle transport in mountain lakes and reservoirs. Annals of Glaciology, 57(71): 232–244

Kargel J S, Leonard G J, Shugar D H, Haritashya U K, Bevington A, Fielding E J, Fujita K, Geertsema M, Miles E S, Steiner J, Anderson E, Bajracharya S, Bawden G W, Breashears D F, Byers A, Collins B, Dhital M R, Donnellan A, Evans T L, Geai M L, Glasscoe M T, Green D, Gurung D R, Heijenk R, Hilborn A, Hudnut K, Huyck C, Immerzeel W W, Liming J, Jibson R, Kaab A, Khanal N R, Kirschbaum D, Kraaijenbrink P D A, Lamsal D, Shiyin L, Mingyang L, McKinney D, Nahirnick N K, Zhuotong N, Ojha S, Olsenholler J, Painter T H, Pleasants M, Pratima K C, Yuan Q I, Raup B H, Regmi D, Rounce D R, Sakai A, Donghui S, Shea J M, Shrestha A B, Shukla A, Stumm D, van der Kooij M, Voss K, Xin W, Weihs B, Wolfe D, Lizong W, Xiaojun Y, Yoder M R, Young N (2016). Geomorphic and geologic controls of geohazards induced by Nepal's 2015 Gorkha earthquake. Science, 351(6269): aac8353

Korup O (2002). Recent research on landslide dams—A literature review with special attention to New Zealand. Prog Phys Geogr, 26(2): 206–235

Krylenko I, Kidyaeva V (2012). Scenarios of evolution of Tangjiashan dammed lake, Sichuan, China. In: Debris Flow Movement Behavior, Numerical Simulation and Hazard Assessment. NSFC-RFBR Bilateral Seminar, Dujuangyan, China

Lee C F, Dai F C (2011). The 1786 Dadu River Landslide Dam, Sichuan, China. In: Evans S G, Hermanns R L, Strom A, Scarascia-Mugnozza G, eds. Natural and Artificial Rockslide Dams. Springer Berlin Heidelberg, 369–388 doi: 10.1007/978-3-642-04764-0_13

Liu N, Zhang J X, Lin W, Cheng W Y, Chen Z Y (2009). Draining Tangjiashan Barrier Lake after Wenchuan Earthquake and the flood propagation after the dam break. Science in China Series E: Technological Sciences, 52(4): 801–809

O'Brien J S, Julien P Y, Fullerton W Y (1993). Two-dimensional water flood and mudflow simulation. J Hydraul Eng, 119(2): 244–261

Owen L A, Kamp U, Khattak G A, Harp E, Keefer D K, Bauer M (2008). Landslides triggered by the 8 October 2005 Kashmir earthquake. Geomorphology, 94(1–2): 1–9

Petrakov D A, Tutubalina O V, Aleinikov A A, Chernomorets S S, Evans S G, Kidyaeva V M, Krylenko I N, Norin S V, Shakhmina M S, Seynova I B (2012). Monitoring of Bashkara glacier lakes (Central Caucasus, Russia) and modelling of their potential outburst. Nat Hazards, 61(3): 1293–1316

Reynolds J M, ed. (2003). Development of glacial hazard and risk minimization protocol in rural environment. Report No. R7816.H, Reynolds Geo-Sciences LTD, UK

Richardson S D, Reynolds J M (2000). An overview of glacial hazards in the Himalayas. Quat Int, 65–66: 31–47

Ruiz-Villanueva V, Allen S, Arora M, Goel N K, Stoffel M (2016).

Recent catastrophic landslide lake outburst floods in the Himalayan Mountain Range. Prog Phys Geogr, doi:10.1177/0309133316658614

Runqiu H (2009). Some catastrophic landslides since the twentieth century in the southwest of China. Landslides, 6(1): 69–81

Schneider J F, Gruber F E, Mergili M (2011). Recent cases and geomorphic evidence of landslide-dammed lakes and related hazards in the mountains of Central Asia. Proceedings of the Second World Landslide Forum, 3−7 October 2011, Rome. doi: 10.1007/978-3-642-31319-6-9

Schuster R L (1993). Landslide dams — A worldwide phenomenon. In: Proceedings Annual Symposium of the Japanese Landslide Society, Kansai Branch, 27 April, Osaka, 1–23

Schuster R L, Alford D (2004). Usoi landslide dam and Lake Sarez, Pamir Mountains, Tajikistan. Environ Eng Geosci, 10(2): 151–168

Shroder J F Jr (1998). Slope failure and denudation in the western Himalaya. Geomorphology, 26(1–3): 81–105

Stefanelli C T, Catani F, Casagli N (2015). Geomorphological investigations on landslide dams. Geoenvironmental Disasters, doi:10.1186/s40677-015-0030-9

Tan W, Hen Q (1992). Study on regional critical rainfall induced debris flow in Sichuan Province. Journal of Catastrology, 7: 37–42 (in Chinese)

Tang C, Zhu J, Chang M, Ding J, Qi X (2012). An empirical-statistical model for predicting debris-flow runout zones in the Wenchuan earthquake area. Quaternary International, 250: 63–73

The United Nations Office for Disaster Risk Reduction. https://www.unisdr.org

Wei F, Hu K, Lopez J L, Cui P (2003). Method and its application of the momentum model for debris flow risk zoning. Chin Sci Bull, 48(6): 594–598

Worni R, Huggel C, Clague J J, Schaub Y, Stoffel M (2014). Coupling glacial lake impact, dam breach, and flood processes: a modeling perspective. Geomorphology, 224: 161–176

Xu Q, Fan X M, Huang R Q, Van Westen C (2009). Landslide dams triggered by the Wenchuan earthquake, Sichuan Province, Southwest China. Bulletin of Engineering Geology and the Environment, 68(3): 373–386

Zemtsov S P, Goryachko M D, Baburin V L, Krylenko I N, Yumina N M (2016). Integrated assessment of socio-economic risks of hazardous hydrological phenomena in Slavyansk municipal district. Nat Hazards, 82(S1): 43–61

Zhang J (2010). Hydrologic analysis and emergency application of barrier lake breaking. Dissertation for PhD degree. Beijing: Tsinghua University (in Chinese)

Zhang S, Xie X, Wei F, Chernomorets S, Petrakov D, Pavlova I, Tellez R D (2015). A seismically triggered landslide dam in Honshiyan, Yunnan, China: from emergency management to hydropower potential. Landslides, 12(6): 1147–1157